La mer 29: 23-34, 1991
Société franco-japonaise d'océanographie, Tokyo

Design of the simple towed vehicle, "EIKO", for the acoustic Doppler current profiler*

Tsutomu HORI**, Masahiko NAKAMURA***, Wataru KOTERAYAMA*** and Arata KANEKO****

Abstract: A fundamental study is described on the dynamics of a submersible towed vehicle with a design which is light and stable to house an acoustic Doppler current profiler. A practical method of calculating the towing cable tension and profile, the attitude and submerged depth of the towed vehicle is proposed. Experimental studies were carried out to obtain the hydrodynamic coefficient of the vehicle to estimate its performance. On-site experiments of the resulting simple and high performance vehicle EIKO confirmed that the purpose of the design was well achieved.

1. Introduction

Ocean tides and currents are important because of their great effect on the global environment, fishery and transportation on the sea. Measured data of the distribution of flow velocity in ocean currents, however, is extremely limited compared with data on the waves, water temperature and salinity because of the lack of a simple and accurate measuring method. Though the conventional geometric electro kinetograph (GEK) is simple and popular, it is not capable of measuring the ocean currents because it is often disturbed by wind-affected local surface flow. A submerged buoy system with current meters is used to obtain a vertical profile of the current, but it is difficult to maintain many submerged buoy systems in the sea and an extremely large scale system is necessary when data is desired over a wide area (TAKEMATSU *et al.*, 1986).

Recently an acoustic Doppler current profiler (ADCP), which can measure the vertical distribution of current velocity in the sea, was developed with the progress of acoustic technology (JOYCE *et al.*, 1982, ISHII *et al.*, 1986, and KANEKO *et al.*, 1990, etc.) This revolutionary instrument instantaneously measures current velocity from the sea surface to a depth of 400 m in each of 128 layers. The measured data of each layer is transformed into the absolute velocity of the current at that depth by automatically calculating the speed of the ADCP relative to the earth if the ocean floor is within acoustic measuring range (400 m). Although this instrument can be directly installed on a research ship, motion of the ship caused by waves have great effect on accuracy of the measurement and installation on a ship hull is difficult. If, however, ocean currents are measured by an underwater towed vehicle on which an ADCP is installed, such a problem can be avoided because the motion of the underwater vehicle is much less than of the research ship (KOTERAYAMA *et al.*, 1988 & 1989), and installation of the towing cable in the ship's hull is very easy.

In this paper, the design of an underwater towed vehicle which carries an acoustic Doppler current profiler and maintains a stable attitude at a constant depth beneath the surface of the water is described, and the results of experiments at sea are reported.

2. Design of underwater towed vehicle

A schematic diagram of the designed system is shown in Fig. 1, in which the flow velocity relative to the towed vehicle is measured by ADCP. The obtained data are transmitted to the research ship through a conductor cable attached to the towing cable and processed in real time by a computer on the research ship. If the water depth is 400m or less, the measured relative velocity of ocean

*Received August 30, 1990
**Computer Science Center, Nagasaki Institute of Applied Science, Aba, Nagasaki 851-01, Japan (Research Institute for Applied Mechanics, Kyushu University during this work)
***Research Institute for Applied Mechanics, Kyushu University, Kasuga, Fukuoka 816, Japan.
****Interdisciplinary Graduate School of Engineering Science, Kyushu University, ditto.

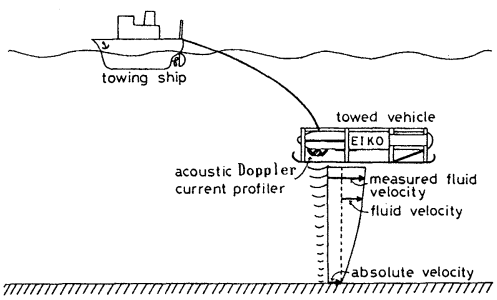

Fig. 1. Concept of the towed vehicle system with an acoustic Doppler current profiler.

currents to the towed vehicle is transformed into the absolute velocity relative to the earth by bottom tracking. If the water depth is over 400m, the measured relative velocity is transformed into absolute velocity using the ship speed which is obtained by the global positioning system (GPS) or the Loran-C navigation system. When the ADCP is located on board the research ship, the motion of the ship induced by surface waves and noise and bubbles generated by the ship's hulll have the serious adverse effects on the instrument's accuracy.

2.1. Design condition and structure

The towed vehicle must be lightweight and small in size for simple operation, but it should have adequate strength. It is also desirable that the vehicle have excess buoyancy so that it can be retrieved if the tow rope is accidentally cut. For accuracy of the profiler, the ship should generate minimum noise and bubbles ; therefore the length of the towing cable should be sufficient to maintain the towed vehicle at a depth of 10m below the sea surface.

In consideration of these design requirements, we decided on a 50m length of cable and a total vehicle length of 2m with a shape as shown in Fig. 2 ; we called it EIKO. The weight of the acoustic current profiler is

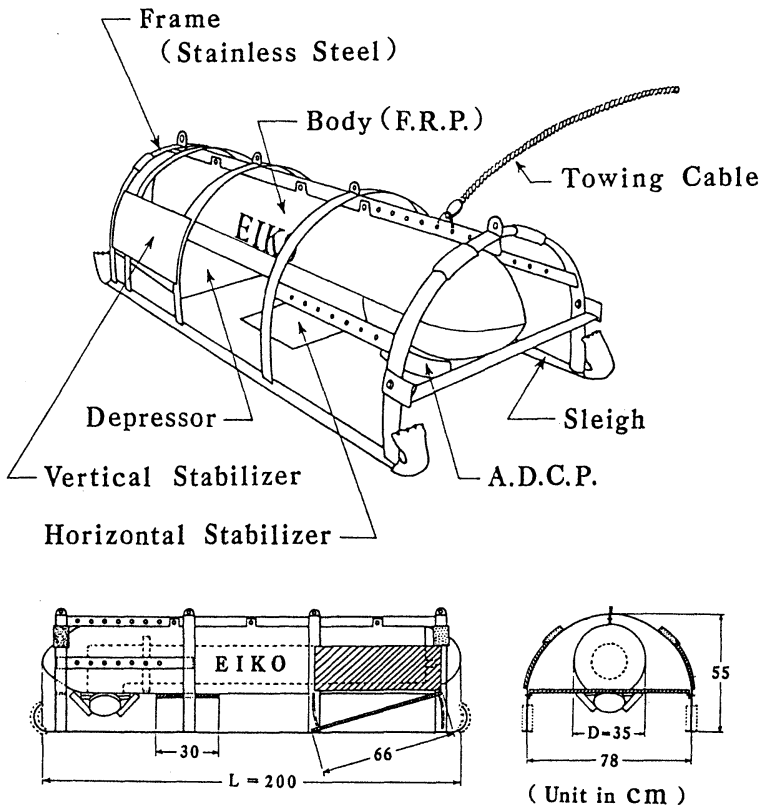

Fig. 2. Design of the towed vehicles (nicknamed EIKO).

about 70kgf, and total weight of the towed system is about 160 kgf ; EIKO's buoyancy is maintained by filling her body with a buoyant material. Though excess buoyancy is an asset in deployment and retrieval, if it is too great the motion of the underwater vehicle is negatively influenced, because its surge and heave is coupled. We therefore designed the vehicle to maintain a neutral buoyancy.

The lower part of the fore body which houses the transducer of the ADCP is open so as not to interfere with the acoustic beam. A depressor made of fiberglass reinforced plastics (FRP) is installed in the aft part of the body for use in lengthening the moment lever to the towed point, and this can be fixed at an arbitrary angle to adjust the lift force to a desired depth. A horizontal stabilizer made of FRP is equipped to prevent pitching and minimize the trim angle. Stainles steel vertical stabilizers minimize the roll and yaw and improve course stability. The main body is also made of FRP and has a shape designed to protect the current profiler and reduce fluid drag. The frame is made of stainless steel acts to further protect the porfiler from the shock of collision with the hull of the towing ship during retrieval and deployment. Two sleigh-type runners have the longitudinal strength and act as buffers when the vehicle is lifted onto the deck of the research ship.

2.2. Experiments on hydrodynamic characteristics in towing tank

Experiments were carried out in a large towing tank created for sea disaster research (L×B×D×d=80×8×3.5×3 m) at the Tsuyazaki Sea Safety Research Laboratory, which is part of the Research Institute for Applied Mechanics of Kyushu University. Hydrodynamic force was measured with a six component dynamometer as shown in Fig. 3. To avoid the free surface effects, the towed vehicle was submerged to the greatest depth possible. The hydrodynamic force acting on the vehicle was are obtained by subtracting the force acting on the strut from the total measured force. During these experiments, the depressor's attack angle β, of which the normal sense is counterclockwise, was fixed

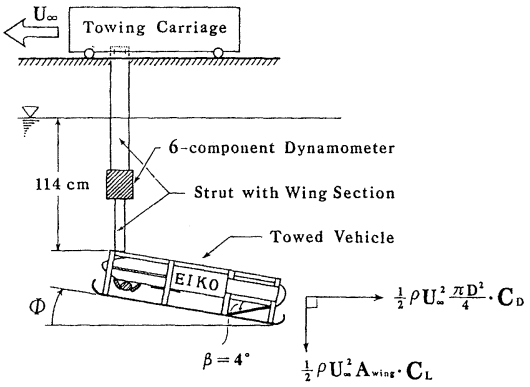

Fig. 3. Experimental setup in the towing tank.

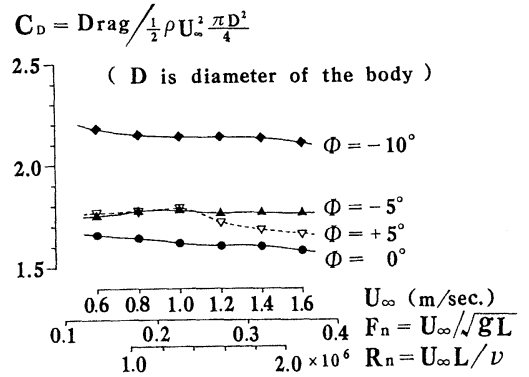

Fig. 4. Drag coefficients C_D of a towed vehicle versus ship speed for various trim angles.

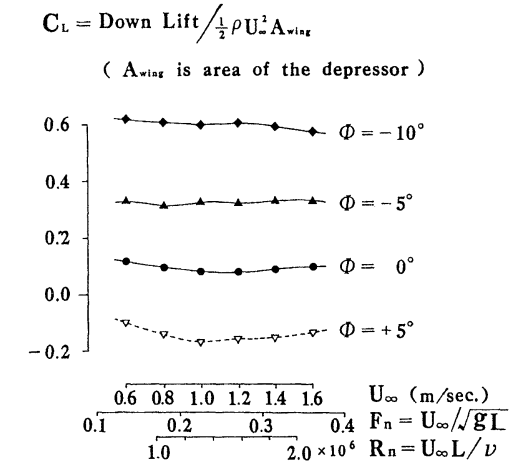

Fig. 5. Down lift coefficients C_L of a towed vehicle versus ship speed for various trim angles.

at 4°. This angle was decided by the conditions that length of the towing cable was 50m and submerged depth of the vehicle was 10m. The calculation method will be described in the next chapter. To examine the dependence of hydrodynamic coefficients upon the vehicle's trim angle Φ, of which the normal sense is clockwise, experiments were done for four cases $\Phi=-5°, 0°, 5°$ and $-10°$. The case of $\Phi=-5°$ corresponded to the actual towed attitude of the vehicle in the ocean. Towing speeds were 0.6~1.6m/s. We define that the direction of drag force is same as that of uniform flow, and that of lift force is perpendicular to the drag force.

Figure 4 shows that the drag coefficient C_D of the vehicle is normalized by the front projectional area $\frac{\pi}{4}D^2$, where D is diameter of the body shown Fig. 2. Figure 5 shows lift coefficients normalized by the wing area of the depressor ; the direction of the lift is positive downwards. These figures indicate that the drag and lift coefficients do not depend on the towing speed U_∞. The drag coefficient C_D is roughly proportional to Φ^2, and the lift coefficient C_L linearly increases with the increase of Φ. However, C_L is not zero at $\Phi=0°$ as shown in Fig. 5, because the vehicle is asymmetrical around the horizontal plane as shown in the front view of Fig. 2. We obtain $C_L=0$ at $\Phi=2°$ by the interpolation in Fig. 5. The reason C_D increases with the increase of trim angle Φ as shown in Fig. 4 is that the induced drags acting on the depressor and horizontal stabilizer increase as shown in Eq. (28) of the next chapter. The value of C_D reaches about 1.6 even at $\Phi=0°$, which means that the drag forces acting on appendages such as the frame of the vehicle, the transducer of the profiler and others account for most of the total drag of the vehicle; the induced drag of the wings is not large at $\Phi=0°$ as denoted in Eq.(28), and the drag coefficient of the main body is estimated as only 0.6. This fact is important because the tension of the towing cable is due primarily to the drag coefficient of the towed vehicle when the weight and length of the cable are small.

Figure 6 shows the heel moment coefficient

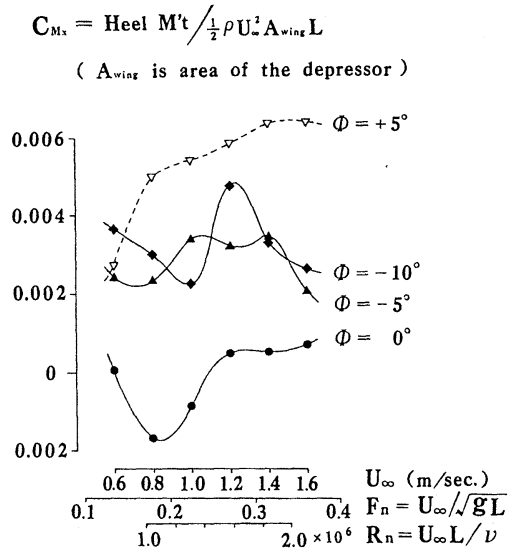

Fig. 6. Heel moment coefficents C_{Mx} of a towed vehicle versus ship speed for various trim angles.

C_{Mx}, which is normalized on the basis of the depressor's wing area and the vehicle's total length. The value of C_{Mx} is usually not zero because of unstable hydrodynamic force. Even small values of C_{Mx} cause the vehicle to capsize in high speed towing when $\overline{BG}$ of the towed vehicle is small, where $\overline{BG}$ is the distance between center of buoyancy and that of gravity. The dependence of C_{Mx} upon the towed speed is unstable as shown in Fig. 6 ; therefore it is actually not possible to adjust the body shape and the angle of wings in order to minimize C_{Mx}. It is thus essential that that the vehicle be stabilized by increasing the restoring force.

3. Theoretical calculation method

3.1. Profile and tension of the towing cable

The towing cable used in this study is short and neutrally buoyant in the water, therefore the dynamics is not important. On the contrary, when the cable is long and heavy, its dynamic analysis is important in estimating the performance of the towed system (Kote-rayama *et al.*, 1988 & 1989). The calculation method of the tension and the profile of a mooring cable, which is neutrally buoyant in the water, was shown by Pode (1951) in his

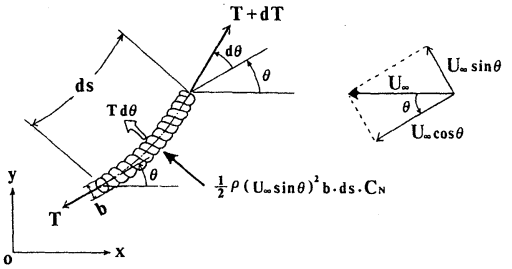

Fig. 7. Forces acting on the differntial element of a zero weight cable in the water.

study, but the same method is not practical for the towing cable. The purpose of this section is to develop the method of calculation for obtaining the depth of submersion.

As shown in Fig. 7, we take the *o-xy* coordinate system in which ds is the differential element of the cable and U_∞ is the uniform flow velocity. The frictional resistance acting along the cable is neglected because it does not contribute to the profile of the cable. We assume that the weight of the cable in the water is zero, then

$$dT=0 \tag{1}$$

Consequently, the tension T along the cable becomes constant

$$T=T_0 \quad (=Const.) \tag{2}$$

Since the drag force acts on the cable in the normal direction and the cable deflects as balancing with its force, the following differential equation is obtained.

$$ds+\lambda\cdot\frac{d\theta}{\sin^2\theta}=0 \tag{3}$$

in which θ is the slope angle of the cable, and λ is the parameter governing the deflection shape of the cable and is defined by

$$\lambda\equiv\frac{2T_0}{\rho U_\infty^2 b\cdot C_N} \tag{4}$$

where b is the diameter of the cable, C_N is the drag coefficient and ρ is the density of the water.

Since $s=0$ at $\theta=\theta_0$, the length s of the cable is obtained as the function of the cable slope θ in the following form by integration with Eq. (3)

$$s=\lambda\cdot(\cot\theta-\cot\theta_0) \tag{5}$$

Equation (5) can be rewritten as :

$$\cot\theta=\tilde{s}+\cot\theta_0 \tag{6}$$

where $\tilde{s}$ is the dimensionless cable length as $\tilde{s}\equiv s/\lambda$. If we use the normalized cable length $\tilde{s}$ and the cable slope θ_0 at the towed vehicle's side, we can estimate the cable slope θ at the end of the side of the research ship.

Since it is not easy to obtain the profile of the cable from Eq.(6), we transfrom the co-odinate system from $(s,\ \theta)$ to $(x,\ y)$. By differentiating the equation of $\cot\theta=dx/dy$, we find that

$$\frac{d\theta}{\sin^2\theta}=-\frac{d^2x}{dy^2}dy \tag{7}$$

and from the definition, we get

$$ds=\sqrt{1+\left(\frac{dx}{dy}\right)^2}dy \tag{8}$$

Eliminating s and θ from Eq. (3) by substituting Eqs. (7) and (8), the profile of the cable can be written in the following form,

$$\tilde{x}=\cosh\{\tilde{y}+\sinh^{-1}(\cot\theta_0)\}-\cosh\{\sinh^{-1}(\cot\theta_0)\} \tag{9}$$

where $\tilde{x}\equiv x/\lambda$, $\tilde{y}\equiv y/\lambda$. From Eq. (9), we find that the profile of the towing cable of neutral buoyancy is a reverse catenary curve, and we can obtain the profile by replacing the horizontal co-ordinate x with the vertical one y.

The submerged depth $\tilde{y}$ of the towed vehicle can be obtained as follows:

$$\tilde{y}=\sinh^{-1}(\cot\theta)-\sinh^{-1}(\cot\theta_0) \tag{10}$$

and substituting Eq. (6) into Eq. (10), we obtain

$$\tilde{y}=\sinh^{-1}(\tilde{s}+\cot\theta_0)-\sinh^{-1}(\cot\theta_0) \tag{11}$$

Eliminating $\tilde{y}$ from Eq. (9) by using Eq. (11), the horizontal distance $\tilde{x}$ between the research ship and towed vehicle can be written in the following form

$$\tilde{x}=\cosh\{\sinh^{-1}(\tilde{s}+\cot\theta_0)\}-\cosh\{\sinh^{-1}(\cot\theta_0)\} \tag{12}$$

Consequently, if the cable length $\tilde{s}$ and the cable slope θ_0 at the end of towed vehicle's side are known, we can estimate $\tilde{y}$, $\tilde{x}$ and θ at the cable end of research ship's side. Equation (11), which explicity gives the submerged

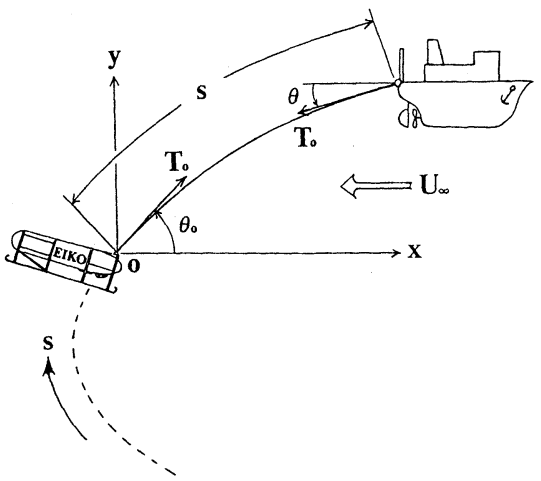

Fig. 8. Deflection shape of the zero weight cable in the water.

depth of the underwater towed vehicle, is especially helpful.

3.2 Attitude and wing angle of the towed vehicle

From the study of the former section we can evaluate the submerged depth of the vehicle when the cable slope at the cable end of the towed vehicle's side is known. In this section we explain the method of estimating the static attitude of the towed vehicle and this gives the condition of the cable end at the towed vehicles's side.

The noations of forces and their directions

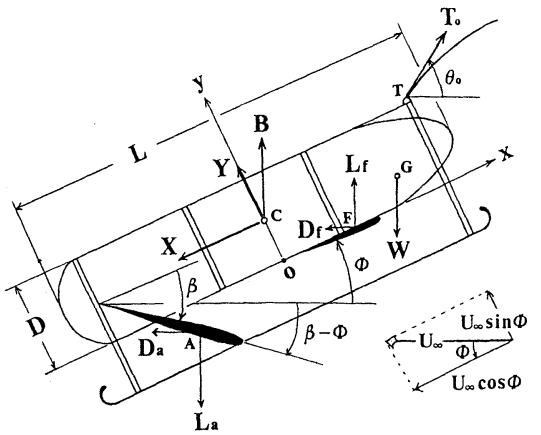

Fig. 9. Coordinate system and forces acting on the towed vehicle.

are defined as shown in Fig. 9. We take a Cartesian co-ordinate system o-xy, where the x-axis is positive in the longitudinal direction and the y-axis is in the transverse direction. As shown in the figure, the vehicle is towed at point T of the bow where the tension is T_0 and the angle is θ_0 at this point. Then the weight W in the water of the acoustic current profiler, the net buoyancy B of the vehicle's body and the drag force X, Y in the x, y direction respectively act on the main body of the towed vehicle. Also, the lift L_a, L_f and the induced drag D_a, D_f act on the depressor and horizontal stabilizer. The towed vehicle thus maintains a condition of static equilibrium as a result of these various forces. Since we consider only a two dimensional problem in the vertical plane, the contribution of the vertical stabilizer is not considered in the static analysis.

The static equilibrium equation of the trim moments about towing point T can be expressed as follows:

$$X\cdot(y_T-y_c)+Y\cdot(x_T-x_c)+B\cdot\xi_c+L_f\cdot\xi_f+D_f\cdot\eta_f+D_a\cdot\eta_a=W\cdot\xi_G+L_a\cdot\xi_a \quad (13)$$

where ξ_j, η_j are the horizontal and vertical distances from the towing point (x_T, y_T) to each point, respectively, and are defined by

$$\left.\begin{aligned}\xi_j&\equiv(x_T-x_c)\cos\Phi-(y_T-y_c)\sin\Phi\\ \eta_j&\equiv(y_T-y_c)\cos\Phi+(x_T-x_c)\sin\Phi\end{aligned}\right\} \quad (14)$$

In Eq. (13), X, Y, L_f, D_f are the function of the speed U_∞, the trim angle Φ of towed vehicle where L_a and Da depend on U_∞, the attack angle $\beta-\Phi$ of the depressor. Then, by Prandtle's lifting line theory L_a, D_a are expressed as the linear or quadratic function of the attack angle $\beta-\Phi$ in the following form, respectively

$$\left.\begin{aligned}L_a&\equiv\tilde{L}_a\cdot(\beta-\Phi)\\ D_a&\equiv\tilde{D}_a\cdot(\beta-\Phi)^2\end{aligned}\right\} \quad (15)$$

We then compare each degree of the term $\beta-\Phi$ and rewrite it in the form of a quadratic equation

$$K_2\cdot(\beta-\Phi)^2-K_1\cdot(\beta-\Phi)+K_0=0 \quad (16)$$

in which K_0, K_1 and K_2 are given, respectively, by

$$\left.\begin{aligned} K_2 &= \tilde{D}_a \cdot \eta_a \\ K_1 &= \tilde{L}_a \cdot \xi_a \\ K_0 &= X \cdot (y_T - y_c) + Y \cdot (x_T - x_c) + B \cdot \xi_c \\ &\quad - W \cdot \xi_G + L_f \cdot \xi_f + D_f \cdot \eta_f \end{aligned}\right\} \quad (17)$$

For Eq. (16) two solutions exist as follows:

$$\beta - \Phi = \frac{K_1 \pm \sqrt{K_1^2 - 4K_0 \cdot K_2}}{2K_2} \quad (18)$$

The coefficient K_2 of Eq. (17) corresponds to the induced drag of the depressor and is much smaller than the other coefficients K_0, K_1 (as shown by Eq. (28) in the next section). Investigating the asymptotic behavior of the solution obtained in Eq. (18) as $K_2 \to 0$, we find that

$$\beta - \Phi \underset{K_2 \to 0}{\sim} \begin{cases} \dfrac{K_1}{K_2} \longrightarrow \infty \\ \dfrac{K_0}{K_1} + \dfrac{K_0^2}{K_1^3} K_2 + O(K_2^2) \end{cases}, \quad (19)$$

The lower solution of the double sign in Eq. (18) is obtained as the perturbation with K_0/K_1, which is the solution to the linear equation putting $K_2 = 0$ in Eq. (16). The upper solution has a large value because it diverges to the order of $1/K_2$ and so is not adopted. Then the angle β of the depressor is obtained as follows:

$$\beta = \Phi + \frac{K_1 - \sqrt{K_1^2 - 4K_0 \cdot K_2}}{2K_2} \quad (20)$$

Thus if the speed U_∞ and the trim angle Φ of the towed vehicle are known, the wing angle β of the depressor is determined as written in Eq. (20). The tension T_0 and the slope θ_0 at the end of the cable are obtained from the equilibrium condition of the forces in the horizontal and vertical directions, respectively.

The equilibrium equation for the forces in each direction are:

$$\left.\begin{aligned} T_0 \cos\theta_0 &= X \cos\Phi + Y \sin\Phi \\ &\quad + D_f + D_a \equiv F_H \\ T_0 \sin\theta_0 &= X \sin\Phi - Y \cos\Phi \\ &\quad + W - B - L_f + L_a \equiv F_V \end{aligned}\right\} \quad (21)$$

From Eq. (21), we can easily determine T_0 and θ_0 in the following form

$$\left.\begin{aligned} T_0 &= \sqrt{F_H^2 + F_V^2} \\ \theta_0 &= \tan^{-1}(F_V/F_H) \end{aligned}\right\} \quad (22)$$

where F_H, F_V are the horizontal and vertical components of T_0 as defined by Eq. (21).

As mentioned above, if the tension T_0 and the slope θ_0 of towing cable are obtained by the analysis of static equilibrium at the side of the vehicle, the submerged depth of the towed vehicle can be obtained. Since we actually need to set the wing angle of the depressor to maintain the required submerged depth of the vehicle to correspond to the towing speed, the calculation must be carried out with an iterative procedure. A chart helpful in estimating the wing angle of the depressor is presented in section 3. 4.

3. 3 Hydrodynamic coefficients of the towed vehicle

In the static analysis of the towed vehicle described in section 3.2, the hydrodynamic coefficients acting on the main body and the two wings need to be determined. Experiments show that the coefficients of drag C_D (Fig. 4) and lift C_L (Fig. 5) for the vehicle are roughly constant versus the towing speed U_∞. In this section, we derive the method for determining the hydrodynamic coefficients acting on the main body and the two wings as functions of the trim angle Φ.

The drag forces X, Y in the x and y-directions acting on the main body of the vehicle (except two wings) are expressed in the following form,

$$\left.\begin{aligned} X &= \frac{1}{2}\rho \cdot (U_\infty \cos\Phi)^2 \cdot \frac{\pi D^2}{4} \cdot C_X \\ Y &= \frac{1}{2}\rho \cdot U_\infty^2 \sin\Phi \,|\sin\Phi|\cdot LD \cdot C_Y \end{aligned}\right\} \quad (23)$$

in which C_x, C_y are the drag coefficients based on the frontal projective areas.

Next, we examine the lifts and the induced drags acting on the horizontal stabilizer (fore) and the depressor (aft).

The lifts of L_f and L_a are respectively noted in the form

$$\left.\begin{aligned} L_f &= \frac{1}{2}\rho U_\infty^2 \cdot b_f c_f \cdot \frac{2\pi k_f}{1 + 2/\Lambda_f} \cdot \Phi \\ L_a &= \frac{1}{2}\rho U_\infty^2 \cdot b_a c_a \cdot \frac{2\pi k_a}{1 + 2/\Lambda_a} \cdot (\beta - \Phi) \end{aligned}\right\} \quad (24)$$

where k_f, k_a are the correction factors from Prandtle's lifting line theory, b_f, b_a are the breadth of the wings, and C_f, C_a are the chord length of the wings, respectively. The aspect ratios of each rectangular wing are defined as $\Lambda_f(=b_f/c_f)$ and $\Lambda_a(=b_a/c_a)$.

The induced drags of D_f, D_a can be written by

$$\left.\begin{aligned} D_f &= \frac{1}{2}\rho U_\infty^2 \cdot c_f^2 \cdot \frac{4\pi}{e_f(2/\Lambda_f)^2}\cdot\Phi^2 \\ D_a &= \frac{1}{2}\rho U_\infty^2 \cdot C_a^2 \cdot \frac{4\pi}{e_a(1+2/\Lambda_a)^2}\cdot(\beta-\Phi)^2 \end{aligned}\right\} \quad (25)$$

in which e_f, e_a are correction factors.

Using the expressions for hydrodynamic forces shown in Eqs. (23), (24) and (25), we obtain the equation of C_D and C_L for the main body with wings.

3.4 Results of computation and discussions

We calculate the submerged depth and trim angle Φ of the towed vehicle shown in Fig. 2 as the function of the angle β of the depressor and the required towing speed U_∞. The results shown in Fig. 10 reveal that the depth of the towed vehicle decreases with the increase of β because the increase of β results in an increse of Φ. This fact indicates that the wing fitted to the vehicle's aft portion performs the role of a controller of the trim rather than a "depressor". Figure 10 also shows that the depth of the vehicle decreases with the increase of U_∞ because of the increase of Φ and the vertical component F_v of the towing tension T_0. This knowledge is helpful when the wing angle and towing speed must be decided to realize a required submerged depth. We determined that wing angle β of the depressor is 4° for the desired submerged depth of 11m at the towing speed $U_\infty=4$ knots, and in this case the trim angle Φ is 2°.

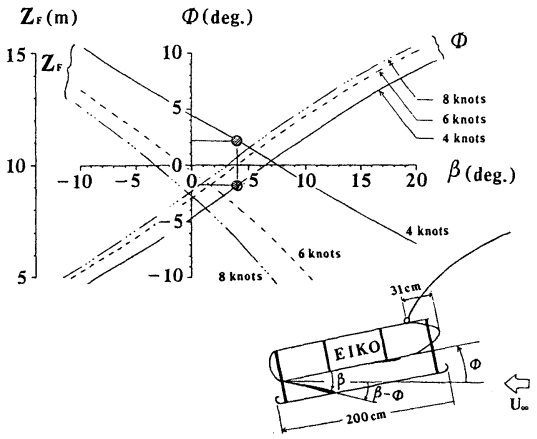

Fig. 10. Trim angles and submerged depths of a towed vehicle versus the attack angles of depressor for various ship speed.

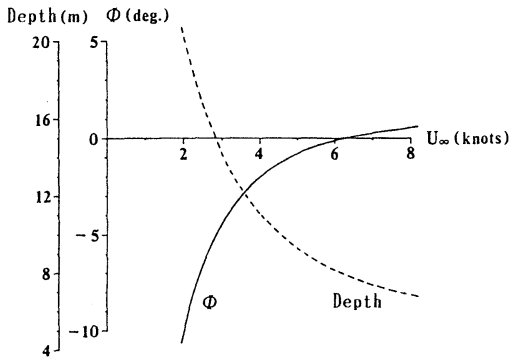

Fig. 11. Trim angles and submerged depths of the towed vehicle versus ship speed in the case of $\beta=4°$.

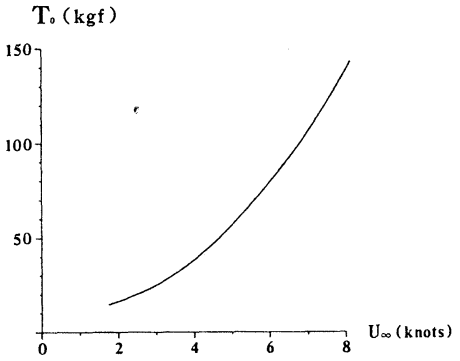

Fig. 12. Tension of the towing cable versus ship speed in the case of $\beta=4°$.

Figure 11 shows the trim angle and the submerged depth of the vehicle versus towing speed U_∞ when β is 4°. The increase of the angle of the depressor and that of the towing speed have the same effect on the submerged depth of the towed vehicle. Both cause the trim angle Φ to increase and it results in a decrease in the depth of submersion. Figure 12 shows the tension T_0 of the towing cable and we find that this cable tension grows in proportion to the square of towing speed.

Since the towed vehicle has an excess buoyancy of 5kgf for the convenience of operation on the sea, it cannot maintain the static stable towing condition appearing in Fig. 11 when the towing speed approaches to zero.

In numerical simulations of motions of the towed vehicle, a quasi-steady solution is introduced in which the variations of attitude and submerged depth of the vehicle and the tension of the towing cable are determined on the basis of the static calculation developed in sections 3. 1 and 3. 2.

4. On-site experiments

Experiments were conducted in the Genkai Open Sea around Oki-no-shima off Fukuoka prefecture in August 1987 to confirm the performance of the towed vehicle "EIKO" on which the acoustic Doppler current profiler was installed. State of sea on the day of the experiments was calm and the height of ocean waves was about 1 m. EIKO was towed by the research ship using a 50 m long and 16 mm diameter towing cable made of polypropylene and with a nearly zero weight in water ; a conductor cable was fitted along the towing cable. Items to be measured were the vertical distribution of the current velocity in the ocean, by the ADCP ; the rolling and pitching angles of EIKO, by a clinometer installed in the ADCP ; the motions of the research ship with six degrees of freedom, by a gyroscopic measuring instrument ; and the tension of the towing cable. The experiments were perfo-rmed under various conditions of towing speed, point of cable attachment and wing angle of the depressor. The confirmed allowable towing velocity of EIKO in these experiments was 2~8 knots ; at higher speed the vehicle capsized because of its unstable heel moment. One example of the experimental results is given ; the vehicle was towed at 4knots with the wing angle of depressor fixed at 4°.

In Fig. 13 the time records of surge, sway and heave of the research ship measured by the gyroscopic measuring instrument suggest that the wave height was about 1 m and the period more than 8.5 sec. Thus the sea weather was calm and the conditions were not the most suitable for the performance test of the towed vehicle, because measurement of the ocean flow by the towed vehicle and the ADCP system would be more informative under severe sea conditions. Figure 14 shows the time records of pitch, roll and yaw of the research ship.

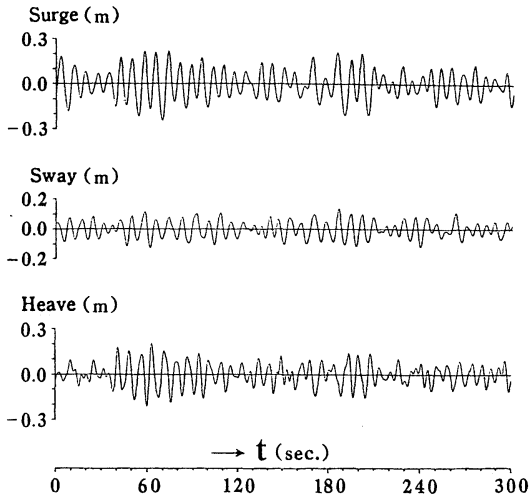

Fig. 13. Time record of the surge, sway and heave motions of the towing ship.

In Fig. 15, we show the time records for the motion of the towed vehicle. The quality of the data obtained is not the best because pitch and roll were measured by a clinometer of the gravitational type and the sampling period of data was about 4 sec because of the limitations in the processing ability of the portable computer on the deck of the research ship.

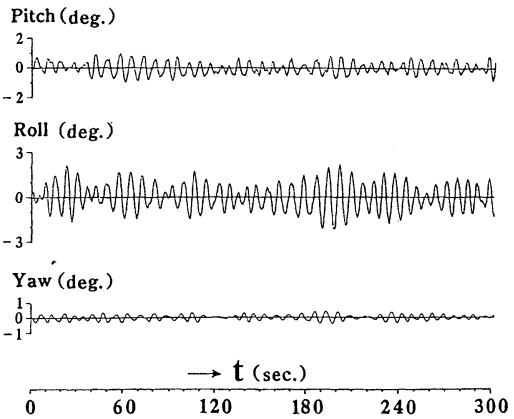

Fig. 14. Time record of the pitch, roll and yaw motions of the towing ship.

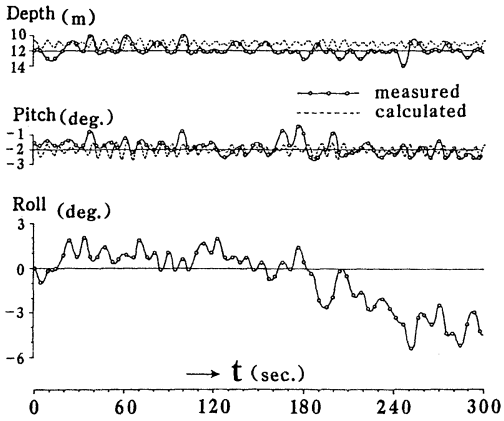

Fig. 15. Time record of the submerged depth and pitch, roll of the towed vehicle.

The characteristics of the oscillation of the towed vehicle, unfortunately, cannot be adequately evaluated with the data at hand. The calculation results of pitching angle shown by the broken line in Fig. 15 were obtained using the quasi-static technique on the basis of the static calculation shown in chapter 3. We have developed a full dynamic calculation method for a vehicle towed by a long and heavy cable, but lengthy computer times is required, making it impractical for calculations on a short, light cable. The calculated pitching angle of the vehicle is obtained by substituting the sum of the ship's mean speed of 4 knots and the fluctuating velocity instead of the steady towing speed U_∞. As shown in Fig. 15, the mean value of pitching angle obtained from the quasi-static calculation is about 2° which coincides with experimental findings. The results of the quasi-static calculations of the variation of pitching angle show good agreement with experiments. We suppose that the large fluctuations in the pitch appearing in the measured values are due to measurement errors because such a phenomenon is not possible in the towed vehicle system.

Experiments show that the rolling angle fluctuates slowly and may be caused by the unstable heeling moment shown in Fig. 6. This problem cannot been avoided so long as the rolling motion is not controlled. The short periodic amplitudes of the pitch and roll are kept within a 1 degree range, so that we can conclude that EIKO is comparatively stable.

The measured value of the submerged depth shown in Fig. 15 is obtained by subtracting the distance between the towed vehicle and the sea bottom measured by ADCP from the sea depth measured by the research ship's depth finder. The value of the submerged depth indicated by the broken line is obtained by quasi-static calculation. From a comparison of calculation and experiment of the submerged depth, we find that the heave fluctuation of the vehicle can be simulated by quasi-static calculation in which the submerged depth varies corresponding to fluctuations of the towing speed caused by surges of the research ship. Although large fluctuations occasionally appear in the measured time record of the submerged depth, theoretical calculation suggests that such a phenomenon cannot occur, and it is supposed that those shown on the record were caused by a measuring error due to the difference in extension of the acoustic beam of ADCP and the depth finder of the rearch ship. The results of the quasi-static calculation on the heave show fairly good agreement with the measured results.

Figure 16 shows the time record of the tension of the towing cable measured at the end of research ship's side. The calculated tension shown by the broken line is obtained by adding the frictional resistance acting along the cable to the time record of the cable tension obtained by quasi-static calculation. The tension variations obtained by the calculation coincide with those of experiments, and we find that the variations in tension are

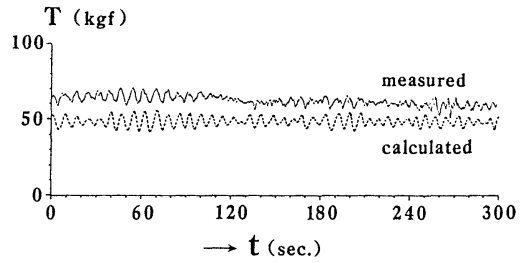

Fig. 16. Time record of the tension of the towing cable.

dependent upon the surging velocity of the research ship. The difference of the mean value of the measured and calculated findings might be due to the effects of an appendage such as the conductor cable which we did not take into account.

Next we show the experimental results of measurements of the ocean flow field by the ADCP installed on EIKO. The depth of the sea area was about 100 m ; current velocities were sampled at every 8 m of the water depth. Figure 17 is an example of the vertical profiles of the velocity and direction of ocean currents measured at latitude 34° 04' north and longitude 129° 32' east. For comparison, measurement data obtained by the submerged buoy system with current meters (ACM) are shown by circles in the figure. The data of the two systems coincide, confirming that the measuring system of ADCP proposed in this paper does provide accurate data of the ocean flow field. In Fig. 18, the time record of the current velocity at every 16 m of water depth is presented. These current vector data were sampled by traversing the Tsushima-East Channel from Tsushima-Izuhara to a spot 10 km to the north of Iki island.

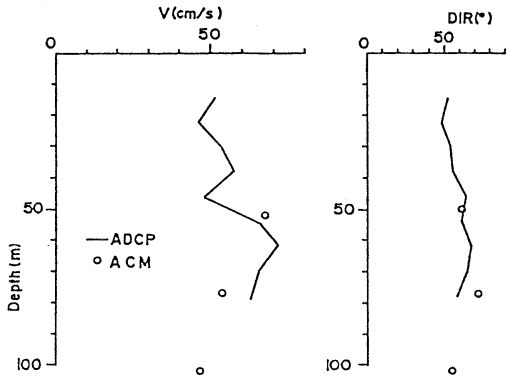

Fig. 17. Vertical profiles of velocity and direction of sea currents obtained by ADCP and ACM at 34°04' N, 129°32'E.

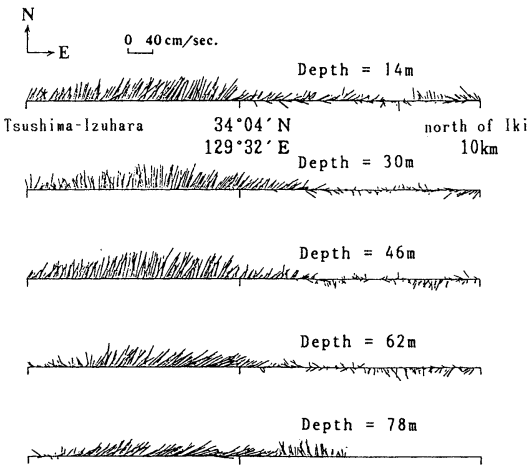

Fig. 18. Vectors of the current sea velocity at various depths.

The system of measurement using a towed vehicle mounted with an ADCP thus can collect ocean data over a wide area with high accuracy. The pitch and roll of the short period of EIKO were kept within a 1 degree range. The motions of EIKO were almost same as those of the research ship, however, because these experiments were done under conditions of following waves and the encounter period was comparatively long. The damping force for motions acting on the towing cable in the region of low frequency, therefore, could not expected. However, theoretical analysis has shown that the motion of the underwater towed vehicle is much less than that of the surface ship in a severe sea state, especially where waves come with high frequency (KOTERAYAMA *et al.*, 1988 & 1989).

5. Concluding Remarks

For the purpose of developing an underwater towed vehicle to carry an acoustic Doppler current profiler, we carried out the fundamental study of a tank test, theoretical calculation and the result was to design a small, lightweight vehicle. On-site experiments confirmed the performance of the vehicle, and we found that the system developed has the ability to carry out practical and informative ocean measurements. We also measured the tension of the towing cable and confirmed that it was within a permitted limit.

The superior characteristics of the towed vehicle suggested by theoretical analyses could not be thoroughly evaluated, however, because the wave height was extremely low and the encounter period comparatively long

in the area of the sea where the experiments were performed. This thus remains to be done in future, but sufficient information was obtained to make the prospects very optimistic.

Acknowledgements

This study was done as part of the Ocean Research Project of the Research Institute for Applied Mechanics in Kyushu University. The on-site experiments described in chapter 4 were carried out in cooperation with the Fukuoka Fishery Station, and we wish to express our gratitude to Captain Mataichi Isobe of the research ship "GENKAI" and to others involved who were so helpful.

References

Ishii, H. *et al.* (1986) : Current Measurement by using Doppler Log, Report of Hydrographic Researches, Japan, No. 21.

Joyce, T. M. *et al.* (1982) : Shipboard Acoustic Profiling of Upper Ocean Currents, Deep-Sea Research, Vol.29, No.7A.

Kaneko, A. *et al.* (1990) : Cross-Stream Survey of the Upper 400m of the Kuroshio by an ADCP on a Towed Fish, Deep-Sea Research, Vol.37, No.5.

Koterayama, W. *et al.* (1988) : A Preliminary Design of a Depth-and Roll-Controllable Towed Vehicle for Ocean Measurements, Jour. Soc. Nav.Arch. Japan, Vol.163.

Koterayama,W. (1989) : Towed vehicle "DRAKE" for the Ocean Measurements and it On-site Experiments in the Kuroshio, Jour. Soc. Nav. Arch. Japan, Vol.165.

Pode, L. (1951): Tables of Computing the Equilibrium Configuration of a Flexible Cable in a Uniform Stream, David Taylor Model Basin Report, Vol.687.

Takematsu, M. *et al.* (1986) : Moored Instrument Observations in the Kuroshio South of Kyushu, Jour. Oceanogr. Soc. Japan, Vol.42.

超音波ドップラー式流速計塔載型の曳航式海中ロボットについて

堀　勉・中村　昌彦・小寺山　亘・金子　新

要旨：従来，海中の流速分布の計測例は，その重要性にも拘わらず簡便で精度の良い計測法が無かったため，波浪・水温・塩分等の観測データに比べて極めて少なかった。最近，音響技術の進歩により，海中流速の鉛直分布を瞬時にして計測し得る超音波ドップラー式音響流速計（acoustic Doppler current profiler: ADCP）が開発された。通常はこの流速計を直接に海洋観測船に搭載し目的の海域を航行して流速を計測するのであるが，波による船体運動やノイズ等の外乱が計測精度に悪影響を及ぼすことと，流速計の船体への固定が大掛かりになるために，専用船でない場合には運用上の問題等が生じ，実用的でなかったと言える。

本報告では，上述の難点を克服をすべく，音響流速計を搭載し制御を行わずして水面下の一定深度を安定な姿勢を保ちながら航走する小型で軽量な水中曳航体（愛称：EIKO）を開発し，昭和62年8月に玄海灘の沖ノ島周辺海域で実施した海上実験に於いてその性能を確認した結果について述べる。また，実際の曳航姿勢や潜航深度が，水槽試験データを用い，曳航索の水中重量を零として近似した準定常的な簡易計算法によって良好に推定できることを示す。